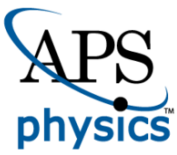

Non-Abelian Quantum Hall Effect in Topological Flat Bands

Yi-Fei Wang, Hong Yao, Zheng-Cheng Gu, Chang-De Gong, and D. N. Sheng

Phys. Rev. Lett. **108**, 126805 — Published 21 March 2012

DOI: 10.1103/PhysRevLett.108.126805

Non-Abelian Quantum Hall Effect in Topological Flat Bands

Yi-Fei Wang[1,2], Hong Yao[3], Zheng-Cheng Gu[4], Chang-De Gong[1,5], and D. N. Sheng[2]
[1] *Center for Statistical and Theoretical Condensed Matter Physics, and Department of Physics, Zhejiang Normal University, Jinhua 321004, China*
[2] *Department of Physics and Astronomy, California State University, Northridge, California 91330, USA*
[3] *Department of Physics, Stanford University, Stanford, California 94305, USA*
[4] *Kavli Institute for Theoretical Physics, University of California, Santa Barbara, California 93106, USA*
[5] *National Laboratory of Solid State Microstructures and Department of Physics, Nanjing University, Nanjing 210093, China*

Inspired by recent theoretical discovery of robust fractional topological phases without a magnetic field, we search for the non-Abelian quantum Hall effect (NA-QHE) in lattice models with topological flat bands (TFBs). Through extensive numerical studies on the Haldane model with three-body hard-core bosons loaded into a TFB, we find convincing numerical evidence of a stable $\nu = 1$ bosonic NA-QHE, with the characteristic three-fold quasi-degeneracy of ground states on a torus, a quantized Chern number, and a robust spectrum gap. Moreover, the spectrum for two-quasihole states also shows a finite energy gap, with the number of states in the lower energy sector satisfying the same counting rule as the Moore-Read Pfaffian state.

PACS numbers: 73.43.Cd, 05.30.Jp, 71.10.Fd, 37.10.Jk

Introduction.—The fractional quantum Hall effect (FQHE) is one of the most fascinating phenomena in interacting quantum many-particle systems. While many Abelian quantum Hall states have been discovered in a two-dimensional electron gas, much effort has been devoted to studies of the non-Abelian quantum Hall effect (NA-QHE) since it was proposed two decades ago [1–10]. One promising experimental candidate for the NA-QHE is the $\nu = 5/2$ state with electrons occupying the second Landau level (LL) [11], while the nature of other candidates like the $\nu = 12/5$ state remains less settled. In addition, the NA-QHE is believed to be possible in fast rotating Bose-Einstein condensates (BEC) [12, 13] and optical lattices with an artificial gauge field [14]. The $\nu = 1$ bosonic Pfaffian state found in the lowest LL [12, 13] is favored by a three-body repulsive interaction [2]. In a lattice model, such repulsive interaction can be realized by imposing the three-body hard-core boson constraint [14] that no more than two bosons on any site are allowed. Interestingly, the three-body hard-core bosons can be mapped to spin $S = 1$ systems, and a NA chiral spin liquid wave function has been proposed recently [15]. The NA-QHE not only is an interesting many-body phenomenon, but also provides a promising platform for implementing topological quantum computation [16].

Recently, systematic numerical works demonstrated convincing evidence of the Abelian FQHE of interacting fermions and hard-core bosons [17–19] in topological flat band (TFB) models [20]. Such TFB models belong to the topological class of the well-known Haldane model [21] with at least one topologically nontrivial nearly-flat band carrying a nonzero Chern number, which is also separated from the other bands by large gaps [20, 22–24]. This intriguing fractionalization effect in TFBs without LLs has stimulated a lot of recent research activities[25–31]. The $\nu = 1/2$ bosonic FQHE found in TFB models for hard-core bosons [18] can also be considered as one example of the long-sought chiral spin states for spin 1/2 system [32]. It is now tempting to take the TFB as a promising testbed to search for more exotic quantum Hall states, possibly with non-Abelian nature.

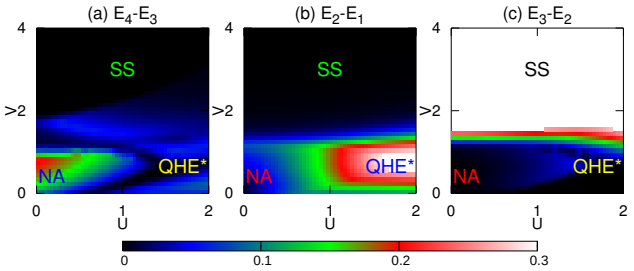

FIG. 1: (color online). Intensity plots of spectrum gaps in U-V phase space for the 20-site lattice at $\nu = 1$. E_1, E_2, E_3 and E_4 denote the energies of the lowest four eigenstates. NA, QHE* and SS label the rough phase regions of NA-QHE, (non-degenerate) quantum Hall phase, and supersolid inferred from all three spectrum-gap plots and other information (see the text).

In this letter, we search for the non-Abelian quantum phase for bosons in TFBs without LLs. Through extensive exact diagonalization (ED) study on the Haldane model with three-body hard-core bosons loaded into a TFB, we find convincing numerical evidence of the $\nu = 1$ bosonic NA-QHE, with the characteristic three-fold quasi-degeneracy of ground states (GSs) on a torus [2, 4, 12], an integer quantized Chern number associated with GSs, and a robust spectrum gap in a finite region of the parameter space. An energy gap is also found to separate the low energy quasihole states from the higher energy ones, indicating the existence of the "zero-energy" sector (for the interacting Hamil-

tonian) [8, 33], as in the Moore-Read Pfaffian state. The number of quasihole states in the lower energy sector also satisfy the same counting rule as the Moore-Read state [7, 8, 19, 34]. We further obtain the quantum phase diagram based on our ED studies and illustrate quantum phase transitions of the NA-QHE phase to other competing states.

Formulation.—We study the Haldane model [21] on the honeycomb lattice with interacting bosons loaded into a TFB [18]:

$$\begin{aligned} H = & - t' \sum_{\langle\langle \mathbf{r}\mathbf{r}' \rangle\rangle} \left[b^\dagger_{\mathbf{r}'} b_{\mathbf{r}} \exp\left(i\phi_{\mathbf{r}'\mathbf{r}}\right) + \text{H.c.} \right] \\ & - t \sum_{\langle \mathbf{r}\mathbf{r}' \rangle} \left[b^\dagger_{\mathbf{r}'} b_{\mathbf{r}} + \text{H.c.} \right] - t'' \sum_{\langle\langle\langle \mathbf{r}\mathbf{r}' \rangle\rangle\rangle} \left[b^\dagger_{\mathbf{r}'} b_{\mathbf{r}} + \text{H.c.} \right] \\ & + \frac{U}{2} \sum_{\mathbf{r}} n_{\mathbf{r}} \left(n_{\mathbf{r}} - 1 \right) + V \sum_{\langle \mathbf{r}\mathbf{r}' \rangle} n_{\mathbf{r}} n_{\mathbf{r}'} \end{aligned} \quad (1)$$

where $b^\dagger_{\mathbf{r}}$ creates a three-body hard-core boson at site $\mathbf{r}$ satisfying $\left(b^\dagger_{\mathbf{r}}\right)^3 = 0$ and $\left(b_{\mathbf{r}}\right)^3 = 0$ [14]; U and V are the two-body on-site and nearest-neighbor (NN) interactions. This model can also be considered as a spin-1 model via the standard mapping from the three-body hard-core bosons to the $S = 1$ spins. It is clear that $U/t \to \infty$ corresponds to the limit of the (two-body) hard-core bosons.

The honeycomb lattice has a unit cell of two sites, and thus has two single-particle bands. Here, we adopt the previous parameters $t = 1$, $t' = 0.60$, $t'' = -0.58$ and $\phi/2\pi = 0.2$, such that a lower TFB is formed with a flatness ratio of about 50 [18]. For our ED study, we consider a finite system of $N_1 \times N_2$ unit cells (total number of sites $N_s = 2N_1N_2$ and total number of single-particle orbitals $N_{\text{orb}} = N_1N_2$ in each band) with basis vectors $\mathbf{a}_1$ and $\mathbf{a}_2$ and periodic boundary conditions. We denote the boson numbers as N_b, and the filling factor of the TFB is thus $\nu = N_b/N_{\text{orb}}$. We diagonalize the system Hamiltonian in each momentum $\mathbf{q} = (2\pi k_1/N_1, 2\pi k_2/N_2)$ sector, with (k_1, k_2) as integer quantum numbers.

The phase diagram.—We first look at the spectrum gaps for a finite lattice with $N_s = 20$ sites at filling $\nu = 1$ as shown by Fig. 1, where E_1, E_2, E_3 and E_4 denote the energies of the lowest four eigenstates, respectively. From the three spectrum gaps $E_4 - E_3$, $E_2 - E_1$ and $E_3 - E_2$, we can obtain rather rich information of the possible phases and related phase diagram. For the $\nu = 1$ NA-QHE, two necessary conditions are: a ground state manifold (GSM) with three quasi-degenerate lowest eigenstates ($E_3 - E_1 \sim 0$), and it is separated from the higher eigenstates by a finite spectrum gap $E_4 - E_3 \gg E_3 - E_1$. From the Fig. 1, it can be seen that both conditions are satisfied simultaneously around the left bottom corner in the U-V space. The right bottom region is characterized by a finite $E_2 - E_1$ gap but a very small $E_3 - E_2$, which is a possible QHE phase (labeled as QHE* with more discussion to follow). While in the upper region with larger V, the energy difference $E_2 - E_1$ almost vanishes and a large $E_3 - E_2$ gap appears, indicating the two-fold quasi-degenerate states. These are consistent with a sub-lattice solid order. Moreover, upon changing boundary phases, the two lowest energy states evolve into the higher energy spectrum, demonstrating its "metallic" nature in additional to its "solid" feature. So we identify this phase as a supersolid (SS) phase [35]. We have also obtained similar results from a larger lattice with $N_s = 24$ sites.

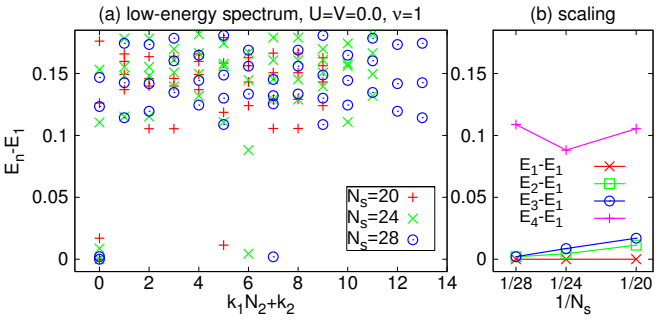

FIG. 2: (color online). (a) Low energy spectrum $E_n - E_1$ versus the momentum $k_1N_2 + k_2$ of the NA-QHE phase for three lattice sizes $N_s = 20$, 24 and 28. (b) Scaling plot of the spectrum gaps in (a).

Low energy spectrum.—For the NA-QHE phase, we would like to check whether the spectrum gap $E_4 - E_3$ holds for other lattice sizes. A few lowest states in each momentum sector of three system sizes with $N_s = 20$, 24 and 28 for the case of $U = V = 0.0$ are shown in Fig. 2(a). The Hilbert subspaces of the $N_s = 28$ lattice have the dimensions of about 700 million (which is about the limit of the current ED method). We can see that, for each system size, there is an obvious GSM with three-fold quasi-degenerate states [two of them in the $(k_1, k_2) = (0, 0)$ sector with very close energies]. The GSM is well separated from the higher energy spectrum by a large gap for all system sizes while the scaling plot of the spectrum gap [Fig. 2(b)] suggests that the gap $E_4 - E_3$ and the three-fold quasi-degenerate GSM of the NA-QHE phase should survive in the thermodynamic limit.

Berry curvature and Chern number.—The Chern number [36] (i.e. the Berry phase in units of 2π) of a many-body state is an integral invariant in the boundary phase space [37, 38]: $C = \frac{1}{2\pi} \int d\theta_1 d\theta_2 F(\theta_1, \theta_2)$, where two boundary phases θ_1 and θ_2 are introduced for the generalized boundary conditions in $\mathbf{a}_1$ and $\mathbf{a}_2$ directions, and the Berry curvature is given by $F(\theta_1, \theta_2) = \text{Im}\left(\left\langle \frac{\partial \Psi}{\partial \theta_2} \middle| \frac{\partial \Psi}{\partial \theta_1} \right\rangle - \left\langle \frac{\partial \Psi}{\partial \theta_1} \middle| \frac{\partial \Psi}{\partial \theta_2} \right\rangle \right)$. For the GSM of NA-QHE phase with $N_s = 24$, the three GSs maintain their quasi-degeneracy and are well separated from the other low-energy excitation spectrum when tuning the boundary phases, indicating the robustness of the NA-QHE phase [Fig. 3(a)]. Moreover, the GSM in the NA-QHE phase

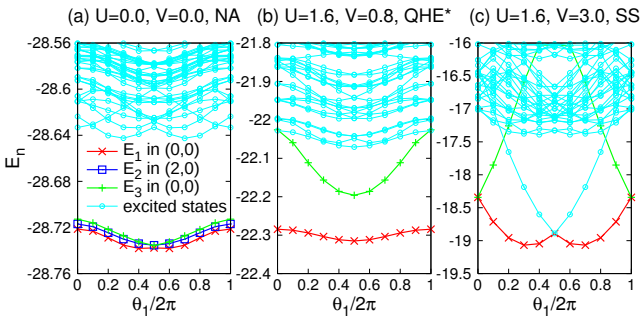

FIG. 3: (color online). Low energy spectra versus θ_1 at a fixed $\theta_2 = 0$ for three phases in the $N_s = 24$ lattice at $\nu = 1$: (a) the NA-QHE phase; (b) the QHE* phase; (c) the SS phase.

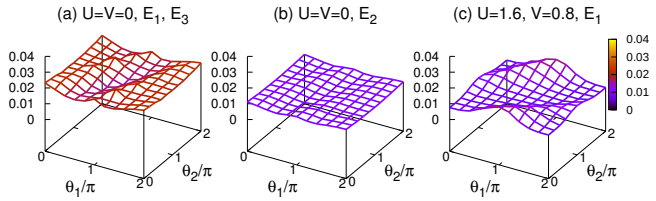

FIG. 4: (color online). Berry curvatures $F(\theta_1, \theta_2)\Delta\theta_1\Delta\theta_2/2\pi$ at 10×10 mesh points for the $N_s = 20$ cases: (a) the 1st and 3rd GSs [(0,0) sector] in the GSM of the NA-QHE phase; (b) the 2nd GS [(1,0) sector] in the GSM of the NA-QHE phase; (c) the single GS of the QHE* phase.

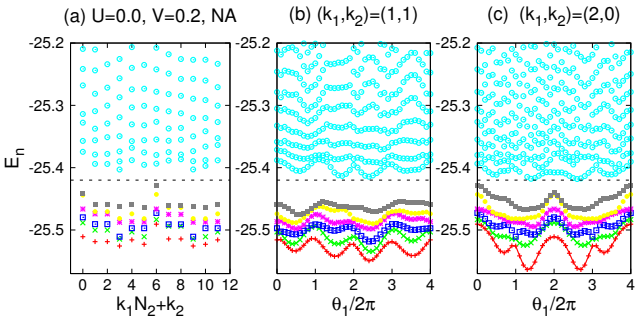

FIG. 5: (color online). (a) Quasihole excitation spectrum in the NA-QHE phase for $N_s = 24$ and $N_b = 11$. (b)-(c) Low energy spectra versus θ_1 at a fixed $\theta_2 = 0$ in two momentum sectors of (a).

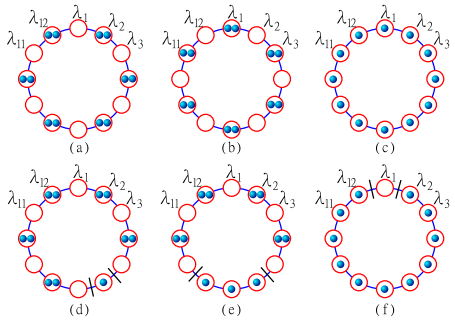

FIG. 6: (color online). Root configurations in the $N_{\rm orb} = 12$ single-particle orbitals: (a)-(c) three GSs (02), (20) and (11); (d)-(f) two-quasihole states with two domain walls (represented by two vertical lines).

shares a total Chern number $C = 3$: e.g. for the $N_s = 20$ cases, we have two GSs of the GSM in the (0,0) sector which contribute the integral Berry phase 4π [Fig. 4(a)], the other GS of the GSM in the (1,0) sector which contributes the integral Berry phase 2π [Fig. 4(b)], and thus the total Chern number of the GSM is $C = 3$. In the possible QHE* phase, the single GS is well separated from other low-energy excitation spectrum when tuning the boundary phases [Fig. 3(b)]. The Berry curvature of the $N_s = 20$ case is shown in Fig. 4(c), which gives rise to a quantized Chern number $C = 1$. On the other hand, for the SS phase, the initial two-fold GS quasi-degeneracy is immediately destroyed when tuning the boundary phases, the two GSs evolve into the higher excitation spectrum. They do not have well-defined Chern numbers since there is no well defined spectrum gap, which indicates a "metallic" feature of this SS phase [Fig. 3(c)].

Quasihole excitation spectrum.—In order to investigate the possible fractional statistics of the NA-QHE state, we study the quasihole excitation spectrum by removing one boson from the $\nu = 1$, and expect two quasiholes of fractional bosonic charge 1/2 [1, 2, 4]. As shown in Fig. 5(a), for a typical NA-QHE state on the $N_s = 24$ lattice, the quasihole spectrum exhibits a distinguishable gap which separates a few lowest states in each momentum sector from the other higher-energy states. For each momentum sector, we check the spectrum gap upon changing boundary phases. For the sectors already with a large gap [e.g. the $(1, 1)$ sector], the spectrum gap is maintained well for all boundary phases with 6 lowest states below the gap as shown in Fig. 5(b). For other sectors [e.g. the $(2, 0)$ sector] where the quasihole gap is less obvious, upon changing boundary phases the spectrum gap becomes clearer and we also find 6 lowest states below the gap as shown in Fig. 5(c). By summing up all 12 sectors together, we have 72 low energy quasihole states in total. We also find similar features for the $N_s = 20$ (and $N_b = 9$) case: there are 5 quasihole states in each momentum sector, and all 10 sectors give 50 low energy quasihole states in total.

The number of low energy two-quasihole states in the NA-QHE phase described above can be heuristically understood from the counting rule based on the generalized Pauli principle [7, 19]. Using the Wannier representation for a TFB [25], a set of $N_{\rm orb} = N_s/2$ periodic single-particle orbitals are formed. Now, let us consider a system with $N_{\rm orb} = 12$ as an example. The generalized Pauli principle that no more than two bosons occupying two consecutive orbitals [7, 8, 19] results in only three GS root configurations in the above orbitals

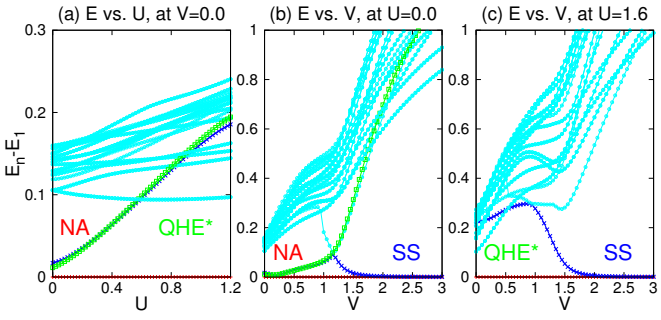

FIG. 7: (color online). Quantum phase transitions when tuning U (or V) with V (or U) fixed for $N_s = 20$: (a) NA-QHE to QHE*; (b) NA-QHE to SS; (c) QHE* to SS.

$|n_{\lambda_1}, n_{\lambda_2}, \ldots, n_{\lambda_{N_{\rm orb}}}\rangle$: (02) $\equiv |020202020202\rangle$, (20) $\equiv |202020202020\rangle$, and (11) $\equiv |111111111111\rangle$ [Figs. 6(a)-(c)]. We now count how many ways we can remove one boson from the above three GS configurations (02), (20) and (11). The boson occupancy of two-quasihole states should be a mixture of two segments of the three GS configurations, with two domain walls each representing one quasihole with 1/2 charge [7]. A simple analysis gives 6 types of configurations with odd number of $1's$: $|\ldots 20|1|020\ldots\rangle$, $|\ldots 20|111|020\ldots\rangle$, $|\ldots 20|11111|020\ldots\rangle$, ..., and $|0|11111111111|\rangle$ [Figs. 6(d)-(f)], where two domain walls (quasiholes) are displayed by two vertical lines |'s. Considering 12 translations of the above 6 states, we finally get the total 72 ($N_{\rm orb}^2/2$ in general) two-quasihole states in exact accordance with our numerical results.

We would like to emphasize that, for the GS obtained numerically, the above mentioned root configurations are not the dominant configurations due to quantum fluctuations just like the other FQHE states in LLs on a torus. But the number of the low energy sector quasihole states in QHE systems is a consequence of the Pauli principle [7, 8, 19] resulting from strong short-range pseudopotentials [9, 33]. Indeed, based on the pattern of zeros classification for FQHE states, the Moore-Read state has a lower energy sector with the same number of quasiholes as obtained in our numerical results [34].

Quantum phase transitions.—When tuning U (or V) with fixed V (or U) away from the NA-QHE region, we observe quantum phase transitions from the NA-QHE to other quantum phases including a possible QHE* and the SS as shown by Fig. 7.

Even though the NA-QHE phase is shown to be remarkably robust in our ED study, we are less certain about the QHE* phase. As shown in Fig. 7(a), if we increase U, two higher energy states from the GSM of the NA-QHE phase will emerge into the excited spectrum, while the evolution of the wave function of the lowest energy state is very smooth. Thus we suspect that the system may have a very long correlation length near the possible QHE* phase, and we conjecture that the spectrum gap above the GS may collapse when the system size becomes very large. We leave this issue to be addressed in future studies.

The SS phase has a two-fold GS quasi-degeneracy, strong intra-sublattice density-density correlations and vanishing inter-sublattice density-density correlations. These observations indicate that the bosons prefer occupying one of the two sublattices. By changing boundary phases, the two GSs of the SS state evolve into the higher energy spectrum, indicating its "metallic" feature besides its solid feature. However if we fix the V as 3.0 and go to a larger $U > 8.0$ (not shown in the phase diagram), the "metallic" character of the SS phase disappears while the solid feature remains indicating the system enters a pure solid phase.

Summary and discussion.—The $\nu = 1$ NA-QHE is characterized by a three-fold quasi-degenerate GSM and a total Chern number $C = 3$ carried by these states. The three-fold quasi-degenerate GSM is only observed for system with even number of bosons ($N_b = 10, 12, 14$) at $\nu = 1$, while it is absent for odd numbers of bosons (e.g. $N_b = 9$ and $N_s = 18$) consistent with the pairing nature for Pfaffian-like states. Interestingly, the $\nu = 1$ NA-QHE is already quite stable with a clear GSM and a large spectrum gap for three-body hard-core bosons without additional interactions ($U = V = 0$). The spectrum gap can even be significantly enhanced with the presence of a small V, which makes it possible for such a state to be realized using optical lattices.

We thank Matthew Fisher, Hong-Chen Jiang, Steve Kivelson, Dung-Hai Lee, and Michael Levin for helpful discussions. DNS thanks Duncan Haldane for stimulating discussions. This work is supported by the US DOE Office of Basic Energy Sciences under Grant No. DE-FG02-06ER46305 (DNS), the NSFC of China Grant No. 10904130 (YFW), the US DOE Grant No. DE-AC02-05CH11231 (HY), the US NSF Grant No. NSFPHY05-51164 (ZCG), and the State Key Program for Basic Researches of China Grants No. 2006CB921802 and No. 2009CB929504 (CDG).

Note added.—After the completion of this work, we became aware of a related work by Bernevig *et al.* [39] addressing the NA-QHE in fermionic TFB systems.

[1] G. Moore and N. Read, Nucl. Phys. B **360**, 362 (1991).
[2] M. Greiter, X. G. Wen, and F. Wilczek, Phys. Rev. Lett. **66**, 3205 (1991); Nucl. Phys. B **374**, 567 (1992).
[3] X. G. Wen, Phys. Rev. Lett. **66**, 802 (1991); Phys. Rev. Lett. **70**, 355 (1993).
[4] N. Read and E. Rezayi, Phys. Rev. B **54**, 16864 (1996); N. Read and E. Rezayi, Phys. Rev. B **59**, 8084 (1999); N. Read and D. Green, Phys. Rev. B **61**, 10267 (2000).

[5] C. Nayak and F. Wilczek, Nucl. Phys. B **479**, 529 (1996).

[6] R. H. Morf, Phys. Rev. Lett. **80**, 1505 (1998); E. H. Rezayi and F. D. M. Haldane, Phys. Rev. Lett. **84**, 4685 (2000).

[7] A. Seidel and D. H. Lee, Phys. Rev. Lett. **97**, 056804 (2006); E. J. Bergholtz, J. Kailasvuori, E. Wikberg, T. H. Hansson, and A. Karlhede, Phys. Rev. B **74**, 081308(R) (2006).

[8] B. A. Bernevig and F. D. M. Haldane, Phys. Rev. Lett. **100**, 246802 (2008); H. Li and F. D. M. Haldane, Phys. Rev. Lett. **101**, 010504 (2008); E. Prodan and F. D. M. Haldane, Phys. Rev. B **80**, 115121 (2009).

[9] F. D. M. Haldane, Phys. Rev. Lett. **107**, 116801 (2011).

[10] M. Levin, B. I. Halperin, and B. Rosenow, Phys. Rev. Lett. **99**, 236806 (2007); S.-S. Lee, S. Ryu, C. Nayak, and M.P.A. Fisher, Phys. Rev. Lett. **99**, 236807 (2007); M. R. Peterson, Th. Jolicoeur, and S. Das Sarma, Phys. Rev. Lett. **101**, 016807 (2008); M. R. Peterson, K. Park, and S. Das Sarma, **101**, 156803 (2008); H. Wang, D. N. Sheng, and F. D. M. Haldane, Phys. Rev. B **80**, 241311 (2009).

[11] R. Willett et al., Phys. Rev. Lett. **59**, 1776 (1987); J. P. Eisenstein et al., Phys. Rev. Lett. **88**, 076801 (2002); J. Xia et al., Phys. Rev. Lett. **93**, 176809 (2004).

[12] N. R. Cooper, N. K. Wilkin, and J. M. F. Gunn, Phys. Rev. Lett. **87**, 120405 (2001).

[13] N. Regnault and Th. Jolicoeur, Phys. Rev. Lett. **91**, 030402 (2003).

[14] B. Paredes, T. Keilmann, and J. I. Cirac, Phys. Rev. A **75**, 053611 (2007); L. Mazza, M. Rizzi, M. Lewenstein, and J. I. Cirac, Phys. Rev. A **82**, 043629 (2010).

[15] M. Greiter and R. Thomale, Phys. Rev. Lett. **102**, 207203 (2009); B. Scharfenberger, R. Thomale and M. Greiter, Phys. Rev. B **84**, 140404(R) (2011).

[16] C. Nayak, S. H. Simon, A. Stern, M. Freedman, and S. Das Sarma, Rev. Mod. Phys. **80**, 1083 (2008).

[17] D. N. Sheng, Z. C. Gu, K. Sun, and L. Sheng, Nature Commun. **2**, 389 (2011).

[18] Y. F. Wang, Z. C. Gu, C. D. Gong, and D. N. Sheng, Phys. Rev. Lett. **107**, 146803 (2011).

[19] N. Regnault and B. A. Bernevig, Phys. Rev. X **1**, 021014 (2011).

[20] E. Tang, J. W. Mei, and X. G. Wen, Phys. Rev. Lett. **106**, 236802 (2011); K. Sun, Z. C. Gu, H. Katsura, and S. Das Sarma, Phys. Rev. Lett. **106**, 236803 (2011); T. Neupert, L. Santos, C. Chamon, and C. Mudry, Phys. Rev. Lett. **106**, 236804 (2011).

[21] F. D. M. Haldane, Phys. Rev. Lett. **61**, 2015 (1988).

[22] X. Hu, M. Kargarian, and G. A. Fiete, Phys. Rev. B **84**, 155116 (2011).

[23] J. W. F. Venderbos, M. Daghofer, and J. van den Brink, Phys. Rev. Lett. **107**, 116401 (2011).

[24] E. Kapit and E. Mueller, Phys. Rev. Lett. **105**, 215303 (2010).

[25] X. L. Qi, Phys. Rev. Lett. **107**, 126803 (2011).

[26] G. Murthy and R. Shankar, arXiv:1108.5501.

[27] Y. M. Lu and Y. Ran, arXiv:1109.0226; J. McGreevy, B. Swingle, and K.-A. Tran, arXiv:1109.1569; A. Vaezi, arXiv:1105.0406; F. Yang, X. L. Qi, and H. Yao, to be published.

[28] T. Neupert, L. Santos, S. Ryu, C. Chamon, and C. Mudry, Phys. Rev. B **84**, 165107 (2011).

[29] D. Xiao, W. Zhu, Y. Ran, N. Nagaosa, and S. Okamoto, Nature Commun. **2**, 596 (2011).

[30] S. A. Parameswaran, R. Roy, and S. L. Sondhi, arXiv:1106.4025.

[31] M. O. Goerbig, arXiv:1107.1986.

[32] V. Kalmeyer and R. B. Laughlin, Phys. Rev. Lett. **59**, 2095 (1987); X. G. Wen, F. Wilczek, and A. Zee, Phys. Rev. B **39**, 11413 (1989); H. Yao and S. A. Kivelson, Phys. Rev. Lett. **99**, 247203 (2007); J. W. Mei, E. Tang, and X. G. Wen, arXiv:1102.2406.

[33] F. D. M. Haldane and D. N. Sheng, to be published.

[34] X.-G. Wen and Z. Wang, Phys. Rev. B **77**, 235108 (2008); X.-G. Wen and Z. Wang, Phys. Rev. B **78**, 155109 (2008)

[35] E. Kim and M. H. W. Chan, Nature (London) **427**, 225 (2004); Science **305**, 1941 (2004).

[36] D. J. Thouless, M. Kohmoto, M. P. Nightingale, and M. den Nijs, Phys. Rev. Lett. **49**, 405 (1982).

[37] Q. Niu, D. J. Thouless, and Y. S. Wu, Phys. Rev. B **31**, 3372 (1985).

[38] D. N. Sheng, X. Wan, E. H. Rezayi, K. Yang, R. N. Bhatt, and F. D. M. Haldane, Phys. Rev. Lett. **90**, 256802 (2003).

[39] B. A. Bernevig and N. Regnault, arxiv:1110.4488.